A comparison of simple rheological models and simulation data of n-hexadecane under shear and elongational flows

C. Baig, B. Jiang, B. J. Edwards,[a] D. J. Keffer, and H. D. Cochran

Department of Chemical Engineering, University of Tennessee, Knoxville, Tennessee 37996-2200

(Received 24 October 2005; final revision received 26 June 2006)

Synopsis

The microscopic origins of five rheological models are investigated by comparing their predictions for the conformation tensor and stress tensor with the same tensors obtained via nonequilibrium molecular dynamics simulations for n-hexadecane. Steady-state simulations were performed under both planar Couette and planar elongational flows, and the results of each are compared with rheological model predictions in the same flows, without any fitting parameters where possible. The use of the conformation tensor for comparisons between theory and experiment/simulation, rather than just the stress tensor, allows additional information to be obtained regarding the physical basis of each model examined herein. The character of the relationship between stress and conformation is examined using model predictions and simulation data. © *2006 The Society of Rheology.* [DOI: 10.1122/1.2240308]

I. INTRODUCTION

One of the primary interests in rheology is to develop both physically and practically useful rheological models that can explain and predict various linear and nonlinear viscoelastic properties of polymeric materials. Although there have been numerous efforts to develop such viscoelastic models for complex liquids using various techniques from the atomistic to the continuum scale, any of the existing models is still far from complete in terms of being able to explain the wealth of complicated phenomena occurring in flowing chain-molecule systems [Bird *et al.* (1987a, 1987b); Morrison 2001; Beris and Edwards (1994)]. However, many models, in particular, ones with sound physical bases rather than purely phenomenological ones, do have merit and can provide some clues that are useful in interpreting complex phenomena and possibly even predicting behavior which is unknown to us. Therefore, it is very important to understand the advantages and disadvantages of the existing rheological models through detailed physical and mathematical analyses and comparison with an extensive suite of experimental and/or simulation data.

In this work, we carry out an analysis on five simple viscoelastic fluid models, each of which has a reasonably sound physical basis: The upper-convected Maxwell (UCM) model, the Rouse model, the extended White/Metzner (EWM) model, the finitely extensible nonlinear elastic (FENE-p) model with the Peterlin approximation, and the Giesekus

[a]Author to whom correspondence should be addressed; electronic mail: bjedwards@chem.engr.utk.edu

model [see, for example, Chapter 8 of Beris and Edwards (1994) for details of these models]. We restrict our attention to these relatively simple models due to the simplicity of the molecular system under consideration: n-hexadecane is well below the entanglement length of linear polyethylene chains, and thus reptation models are not going to apply to this situation. The question then arises: Why should *any* of these rheological models for polymers, reptation or not, apply to the fairly short-chain n-hexadecane, and, even if they did, what useful information can be gleaned from examining them?

The answer to the above-stated question is one of time scales. Indeed, many models commonly used for polymer rheology were actually derived for some other physical system. For example, the UCM model was developed by applying Oldroyd's contravariant deformation derivative [Oldroyd (1950)] to the model derived by Maxwell (1867) for a dilute gas! The operative time scale for this physical system is on the order of 10^{-15} s. Yet, this model has played a major role in the development of polymeric flow theory on many different time scales. Furthermore, this model is the limiting case for vanishing strain rate for many other viscoelastic fluid models. It corresponds to the Hookean dumbbell model derived through kinetic theory (Bird *et al.* 1987b). In fact, the multiple-mode version is still the primary fitting model for storage and loss moduli in small-amplitude oscillatory flow experiments for all sorts of viscoelastic fluids. As another example, consider the Oldroyd-B model. This model was developed by applying Oldroyd's contravariant deformational derivative to the model introduced by Jeffreys (1924) to describe the motion of the Earth's tectonic plates on geological time scales (10^{15} s). Again, despite the overwhelming difference in time scales of polymers compared to the Earth's mantle, this model has been used commonly in viscoelastic flow calculations.

In hexadecane, the intrinsic time scale is very small relative to those of typical polymer solutions and melts. According to our equilibrium and nonequilibrium simulations, described below, the longest (rotational or Rouse) relaxation time of n-hexadecane is about 190 ps. Thus, for all common experimental procedures, this fluid is Newtonian for all practical purposes. However, an advantage of simulation is that impractical situations can often be investigated with relative ease, and, in this case, it is possible to exceed the strain rate (reciprocal of the Rouse time) at which point significant non-Newtonian flow characteristics might be expected to appear. After all, even a dilute gas, according to Maxwell, will exhibit viscoelastic characteristics under the right conditions.

All of the simple models examined herein reduce to the UCM model under the appropriate conditions, generally when the strain rate vanishes. As described below, each model extends the UCM model by incorporating an additional ansatz for the motion of the chain molecules comprising the system. Although these models were developed for polymeric fluids with time scales much larger than hexadecane, there is no reason to expect that the inherent physics contained therein is not also applicable on the much smaller time scale. It is thus natural to examine how well these simple models compare to simulated results of short-chain molecules under shear and planar elongational flows at high strain rates. Whether or not the results are directly applicable to entangled polymers is not the issue here; they are probably not applicable. Nevertheless, the simulation results presented herein do offer significant clues as to the nature of the viscoelastic responses of the various models relative to the structure of the chains that they purportedly represent. For instance, possible issues to resolve are: Does the maximum chain length in the FENE-p model correspond to the actual length of the chains, and does the anisotropic mobility tensor of the Giesekus model correspond to actual physics? These questions can be addressed in a systematic fashion using nonequilibrium molecular dynamics (NEMD) simulations.

In the following analysis, instead of using only the stress tensor or material functions

for comparison between theory and experiment/simulation, we employ primarily the conformation tensor in analyzing the predictive capabilities of each model. Of course, it is difficult to measure the conformation tensor directly during experimentation, but it is very easy to calculate it during simulation. The dimensionless conformation tensor, $\tilde{\mathbf{c}}$, is defined herein as

$$\tilde{\mathbf{c}} = \langle 3\mathbf{RR}/\langle R^2\rangle_{\text{eq}}\rangle, \tag{1}$$

where $\mathbf{R}$ represents the end-to-end vector of chain. The angular brackets represent the time average of the system trajectory, and the subscript eq stands for the equilibrium state. Notice that at equilibrium, $\tilde{\mathbf{c}}$ reduces to the unit tensor.

Another aspect of this work is that we use the steady-state simulation data not only under shear, but also under elongational flow. This is another advantage of simulation over experiment, since it is extremely difficult to obtain the steady-state experimental data under elongation. This is considered essential since rheological models are, in general, built without regard to a specific type of flow, and thus the test of models using data under shear flow only is not as informative.

II. SIMULATION DETAILS

The simulation data under planar Couette flow (PCF) and planar elongational flow (PEF) were obtained by performing (constant particle number, volume, and temperature) NVT NEMD simulations using the *p*-SLLOD algorithm incorporating the Nosé-Hoover thermostat (Nosé 1984a, 1984b; Hoover 1985). The equations of motion for this system, as well as all of the pertinent simulation details, are described elsewhere (Cui *et al.* 1996a; Baig *et al.* 2005a, 2005b; Edwards *et al.* 2005). The united atom model known as the Siepmann, Karaboni, and Smit (SKS) model, [Siepmann *et al.* (1993)] was used to describe n-hexadecane. This model does an excellent job of describing the thermophysical properties of liquid and gaseous n-alkanes under quiescent conditions (Siepmann *et al.* 1993; Ionescu *et al.* 2006), and has been shown to reproduce experimental viscosity measurements of Newtonian n-alkanes (Cui *et al.* 1996b).

In this work, we employed 162 molecules of hexadecane ($C_{16}H_{34}$) for both PCF and PEF. The state point in this study is exactly the same as that used by Cui *et al.* (1996a) for shear flow: The temperature is $T=323$ K, and the density is $\rho=0.7530$ g/cm^3. We employed the same range of strain rates for PCF and PEF: $0.002 \leqslant \dot{\gamma}(m\sigma^2/\varepsilon)^{1/2}$, $\dot{\varepsilon}(m\sigma^2/\varepsilon)^{1/2} \leqslant 1.0$. Here, $\dot{\gamma}$ and $\dot{\varepsilon}$ denote the shear and elongation rates, respectively, m is mass of the CH_2 group, and σ and ε, respectively, are the size and energy parameters of the CH_2 group in the Lennard-Jones potential in the SKS model. The lowest strain rate is small enough for the system to lie within the linear viscoelastic regime. The highest strain rate is well below the point where any thermostat artifacts are known to occur (Cui *et al.* 1996a; Baig *et al.* 2005b). Statistical error bars for the simulation data can be found in Baig *et al.* (2005b) and Cui *et al.* (1996a).

III. VISCOELASTIC MODELS

All five viscoelastic models studied in this work contain two common parameters, the (longest) primary relaxation time of the system, λ, and the concentration of chains, n. (See the Appendix for the detailed equations for each of the five models.) From the state point of the simulation, we know that $n=0.002/\text{Å}^3$. An equilibrium molecular dynamics simulation reveals that $\lambda=191$ ps, which was obtained using the time correlation function of the chain end-to-end unit vector (Cui *et al.* 1996a; Doi and Edwards 1986; Baig *et al.* 2005b). This value agrees very well with the one obtained from NEMD simulations for

the Rouse time obtained from the reciprocal value of the strain rate for the onset of strain-thinning behavior in planar elongational flow (Baig *et al.* 2005b). These values of λ and n are used to obtain the predictions of each model. Therefore, the two linear models (the UCM and Rouse models) containing only λ and n, in fact, have no fitting parameters whatsoever. The other three nonlinear models (the EWM, FENE-p, and Giesekus models) contain one additional parameter. The nonlinear parameters, $k=-36.2$ for PCF and -4.98 for PEF, a shear (tension)-thinning exponent in the EWM, and $\alpha=0.882$ for PCF and 1.00 for PEF, a factor accounting for anisotropic drag forces in the Giesekus model, were obtained by fitting one ($\tilde{c}_{xy}$ for PCF) or two ($\tilde{c}_{xx}$ and $\tilde{c}_{yy}$ simultaneously for PEF) components of $\tilde{\mathbf{c}}$ to the simulation data. In the FENE-p model, the nonlinear parameter, b, the maximum chain extension, can also be obtained from simulation, as will be discussed later. Ergo, the FENE-p model also has no fitting parameters.

Note that the parameter k of the EWM model is significantly different in PCF than in PEF. One would expect that this parameter should be the same in both types of flow if the underlying physical concept of the model was realistic. This parameter of the EWM model quantifies the degree of change induced in the fluid's relaxation time due to the orientation induced by the imposed flow field. Although perhaps reasonable for polymeric fluids, for a short-chain molecule, such as hexadecane, one would expect that this parameter would not have much of an effect on the system relaxation time. The large difference in its value between the two types of flow fields seems to invalidate the model for short-chain molecular systems, since the relaxation time of the stretched molecules cannot be dramatically altered by the flow field. Nevertheless, we shall present the results from this model below for didactic purposes.

From the perspective of the Hookean dumbbell model (which is equivalent to the UCM model), the drag coefficient, ζ, can be calculated from equilibrium simulations through the formula $\zeta=4K\lambda$ (Beris and Edwards 1994). For hexadecane, the spring constant, K, was calculated as 3.05×10^{-3} kg/s^2, which gives a value for ζ of 2.33×10^{-12} kg/s.

For several of the models investigated herein, analytical solutions for the conformation tensor and material functions for PCF and PEF can be derived. In the case that analytical solutions could not be derived, the model equations were solved numerically using the Newton-Raphson method (Press *et al.* 1992). The technique we employed to optimize the model parameters (for the EWM and Giesekus models) to simulation data was the Nelder and Mead downhill simplex method (NMDSM) (Press *et al.* 1992). [For more details concerning the numerical methodology, see Jiang *et al.* (2004)].

IV. COMPARISONS OF MODELS AND SIMULATION DATA

With these results for $\tilde{\mathbf{c}}$ and the material functions for each model, let us compare the predictions of the models with the simulation data. Figure 1 shows the prediction of each model for the conformation tensor under PCF. The results for $\tilde{c}_{xy}$, which are directly related to the shear viscosity, are shown in Fig. 1(a). As expected, both the UCM and Rouse models are shown to predict data in the linear regime only, which is readily understood from Eqs. (A3) and (A10) for these models, respectively. However, as two-parameter models without any fitting parameters, their predictions for the linear data are still reasonably good and considered useful in practical applications. A noticeable thing in Fig. 1(a) is that, quantitatively, the Rouse model shows an excellent prediction, much better than the UCM model. It has been noted previously that the Rouse model works surprisingly well for short-chain molecular systems [Kremer and Grest 1990]. This apparent result leads to an important conclusion: Comparing $\tilde{c}_{xy}$ in Eqs. (A3) and (A10), it

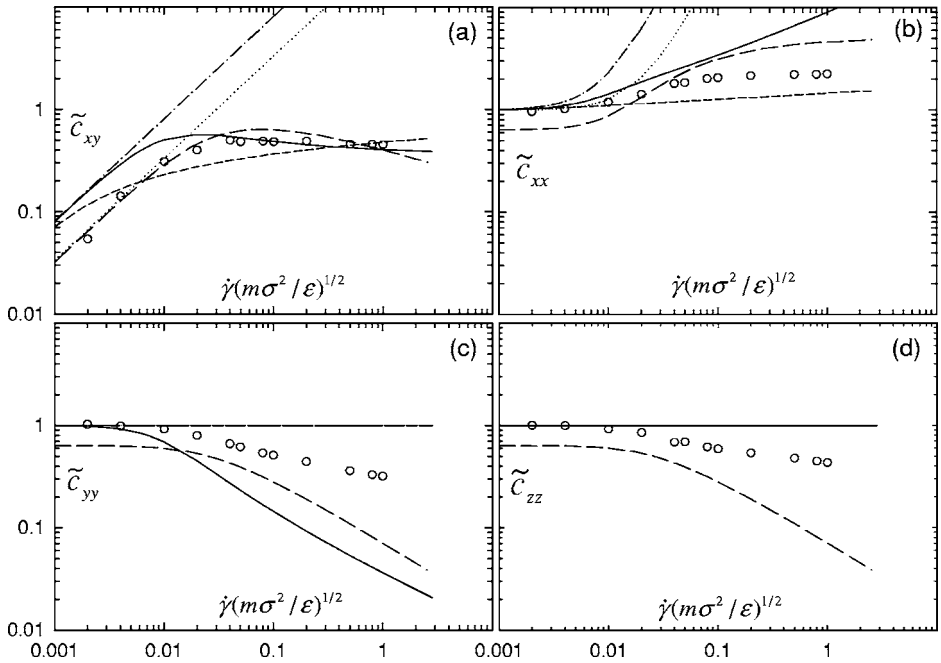

FIG. 1. Comparison between the model predictions and simulation data for the conformation tensor versus shear rate under PCF: (a) $\tilde{c}_{xy}$, (b) $\tilde{c}_{xx}$, (c) $\tilde{c}_{yy}$, and (d) $\tilde{c}_{zz}$. The circles and lines, respectively, represent the simulation data and the model predictions: the UCM model (the dashed-dotted lines), the Rouse model (dotted lines), the EWM model (short-dashed lines), the FENE-p model (long-dashed lines), and the Giesekus model (solid lines). Notice that (c) and (d) appear to have fewer lines due to the overlap between lines.

is seen that λ in the UCM model is quantitatively not the same as that in the Rouse model, but is different by a factor of $(4/\pi^2)\Sigma_{p:\text{odd}}1/p^4(\approx 0.41)$. That is, λ(UCM) is equal to approximately $0.41\times\lambda$(Rouse). From the result shown in Fig. 1(a), it would be reasonable to conclude that λ in the Rouse model, and not λ in the UCM model, represents the "true" primary relaxation time of the physical system. {In fact, such an excellent prediction of the Rouse model is also observed in other short chain systems, such as $C_{10}H_{22}$ and $C_{24}H_{50}$ [Baig (2005)]}.

Now let us look at the predictions of the nonlinear models in Fig. 1(a). The EWM model is seen to predict the nonlinear behavior of $\tilde{c}_{xy}$ to some extent, but does not perform well quantitatively. Over the range of shear rates examined herein, the end-to-end extension of the hexadecane chains changes by approximately 50% from the equilibrium value (Baig *et al.*, 2005b). The EWM model underestimates the degree of molecular extension for these short chains. Although it is possible that the concept of a conformation dependent relaxation time might apply well to longer chain polymers, for short chains, it appears that the relatively small value of the maximum possible chain extension is incompatible with the required degree of change in the relaxation time.

The best prediction of $\tilde{c}_{xy}$ over the whole range of shear rates is produced by the FENE-p model. This is quite remarkable since there are no fitting parameters in this model. It is seen from this result that the non-Gaussian behavior of chains represented by the parameter b in the FENE-p model plays an important role in correctly predicting the physical phenomena of this short-chain system under flow. Another point worthy of considering in Fig. 1(a) is that the FENE-p model has the capability to predict the concave shape of $\tilde{c}_{xy}$, passing through a maximum at an intermediate shear rate. Here, we

chose the FENE-p maximum extension length to be that of the chain in the extended zig-zag conformation, with all bonds and bond angles at their equilibrium values. Of course, b would be larger if the bonds and bond angles were stretched out further, but the value chosen seems to give an accurate description of the FENE dynamics.

Although it is not as good as the FENE-p model, the Giesekus model is shown to predict $\tilde{c}_{xy}$ reasonably well. However, considering that the initial slope of the predicted curve is almost the same as that of the UCM model, the apparent discrepancy of the Giesekus model is presumed to come mainly from the choice of λ in the UCM model rather than its physical basis. (This argument seems to be understandable by considering in the figure that a slight change of the initial slope of the curve would make the Giesekus prediction as good as the FENE-p.) At higher shear rates, the Geisekus model exaggerates the extension of the chains; however, the qualitative features are well described. This lends credence to the concept that anisotropic chain alignment gives rise to an anisotropic mobility tensor: As the chains stretch and align under increasing flow strength, they exhibit enhanced molecular extension/compression relative to undeformed molecules. Again, however, it seems that the hexadecane molecules experience a much smaller anisotropic effect due to the relatively short length of the chains.

The model predictions for $\tilde{c}_{xx}$ are shown in Fig. 1(b). According to Eqs (A3) and (A10), both the UCM and Rouse models predict a quadratic dependence of $\tilde{c}_{xx}$ on the shear rate. Quantitatively, however, the prediction of the Rouse model for the data in the linear regime in Fig. 1(b) is seen to be excellent and much better than that of the UCM model. The FENE-p model again appears to be the most satisfactory in predicting the nonlinear behavior of $\tilde{c}_{xx}$. Notice, however, that the FENE-p model does not predict unity, but $(b-3)/b$ of $\tilde{c}_{xx}$ (in fact, $\tilde{c}_{yy}$ and $\tilde{c}_{zz}$ as well) for $\dot{\gamma}\to 0$, which is readily understood from Eq. (A17). The reason for this discrepancy is that the definition of the dimensionless conformation tensor, Eq. (1), is inconsistent with the FENE-p model. For this model, the form of the dimensionless conformation tensor which should be applied to the simulation data is

$$\tilde{\mathbf{c}} = \left\langle \frac{3}{R_0^2}\left(\frac{R_0^2}{\langle R^2\rangle_{\text{eq}}} - 1\right)\mathbf{RR}\right\rangle. \tag{2}$$

Note that this expression reduces to Eq. (1) when R_0 is relatively large compared with $(\langle R^2\rangle_{\text{eq}})^{1/2}$, i.e., for long-chain molecules; hence, this discrepancy is only noticeable for small molecules, such as hexadecane. To simplify the discussion henceforth, and to keep the number of figures at a minimum, only Eq. (1) is applied to the simulation data; however, the reader should mentally shift the FENE-p simulation data accordingly.

For $\tilde{c}_{yy}$ and $\tilde{c}_{zz}$, shown in Figs. 1(c) and 1(d), respectively, both the UCM and Rouse models predict unity. Therefore, nonunit values of $\tilde{c}_{yy}$ and $\tilde{c}_{zz}$ are considered as nonlinear viscoelastic properties. For $\tilde{c}_{yy}$, the EWM model predicts unity, as do the linear models. The Giesekus model, however, is shown to predict qualitatively the decrease of $\tilde{c}_{yy}$ with increasing shear rate, but does not do so quantitatively. Overall, the FENE-p model appears to provide the closest description of the degree of decrease of $\tilde{c}_{yy}$ as a function of shear rate up to intermediate values. [This is more apparent after mentally shifting up $\tilde{c}_{yy}$ by the factor $(b-3)/b$.] For $\tilde{c}_{zz}$, all models except the FENE-p predict unity for $\tilde{c}_{zz}$, regardless of the value of shear rate. The FENE-p model predicts not only the nonunit value of $\tilde{c}_{zz}$, but also the overall nonlinear behavior, fairly well. Notice from Eq. (A17), however, that the FENE-p prediction for $\tilde{c}_{yy}$ is the same as that for $\tilde{c}_{zz}$, which leads to a zero-value of the second normal stress coefficient, as discussed below.

Summarizing, while the linear viscoelastic behavior of the conformation tensor under

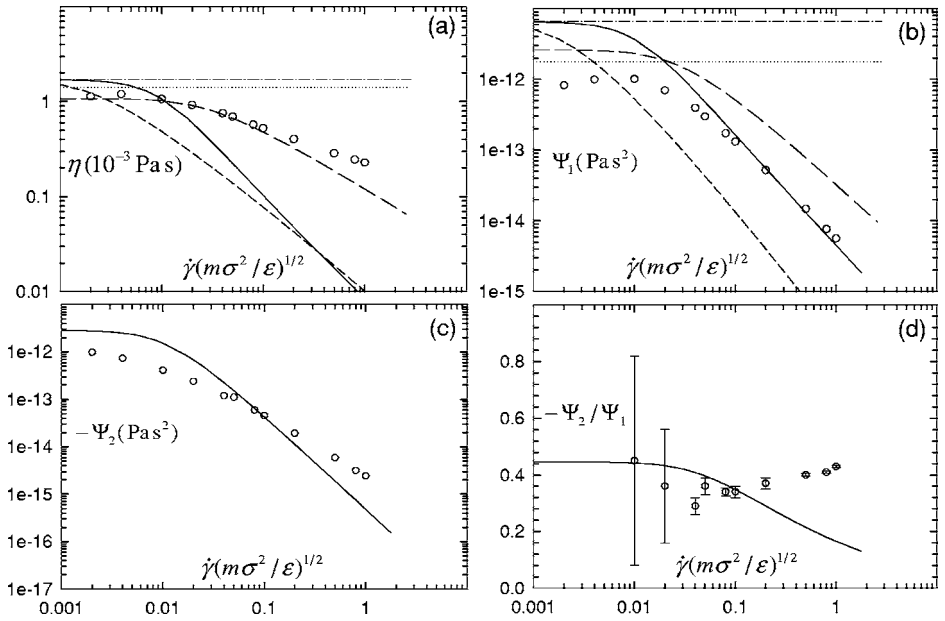

FIG. 2. Comparison between the model predictions and simulation data for the steady-state material functions in PCF: (a) Shear viscosity, (b) first normal stress coefficient, (c) second normal stress coefficient, and (d) the ratio of second to first normal stress coefficients. The symbols and lines represent the same quantities as in Fig. 1. Note that all models except the Giesekus predict a vanishing second normal stress coefficient.

PCF is predicted very well by the Rouse model, the overall linear and nonlinear behaviors are best predicted by the FENE-p model. This is rather remarkable, considering that there are no fitting parameters in the FENE-p model. The Giesekus model appears to be fairly satisfactory, although not as good as the FENE-p model. In contrast, the EWM model does not appear to be very good, compared with the other two nonlinear models.

Now, let us look into the model predictions for the steady-state material functions under PCF. As shown in Fig. 2(a), the zero-shear viscosity appears to be reasonably well predicted by the UCM model. However, a more satisfactory result quantitatively is achieved by the Rouse model, which again demonstrates the superiority of the Rouse model to the UCM model in predicting the linear viscoelastic properties of chain molecules. Despite the fact that the UCM model is considerably worse than the Rouse model in predicting $\tilde{c}_{xy}$, its prediction for the zero-shear viscosity appears to be better than one would have expected from Fig. 1(a). This apparent contradiction stems from the canceling effect between two "incorrect" parameter values, λ and n, in the UCM model. Recall that $\lambda(\mathrm{UCM}) = 0.41\,\lambda(\mathrm{Rouse})$. Taking into account the difference between the λ's in the two models, the comparison of the shear viscosity between Eqs. (A4) and (A11) shows that n in the UCM model is different from that in the Rouse model by a factor of about 2. The quantitatively correct prediction of the Rouse model for both $\tilde{\mathbf{c}}$ and zero-shear viscosity proves that both λ and n in the Rouse model are the correct values, but those in the UCM model are not. Now, it can be understood that the apparently good prediction of the zero-shear viscosity by the UCM model has occurred due to the canceling effect between λ and n with factors of approximately 0.4 and 2, respectively. However, even with the canceling effect, the UCM model still results in a larger value of the zero-shear viscosity by a factor of $12/\pi^2$ than the Rouse model. [This can be noticed in Fig. 2(a)].

Regarding the shear-thinning behavior in Fig. 2(a), neither the EWM nor the Giesekus

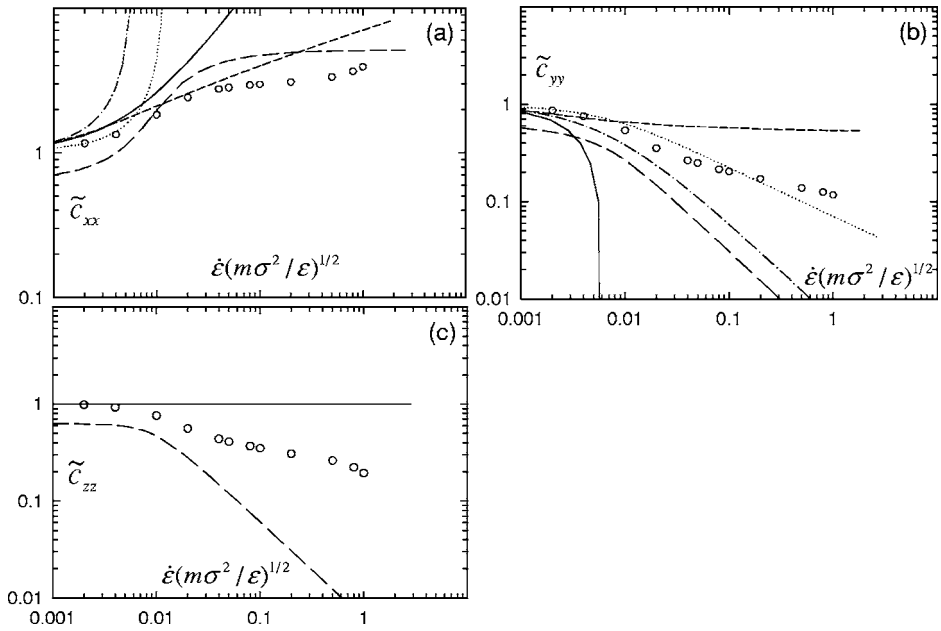

FIG. 3. Comparison between the model predictions and simulation data for the conformation tensor vs elongation rate under PEF: (a) $\widetilde{c}_{xx}$, (b) $\widetilde{c}_{yy}$, and (c) $\widetilde{c}_{zz}$. The symbols and lines represent the same quantities as in Fig. 1.

models satisfactorily describes either the zero-shear viscosity or the degree of shear thinning. An excellent prediction is observed by the FENE-p model for both the linear and nonlinear regimes, although there appears to be a little discrepancy at high shear rates.

In Fig. 2(b), we plot the first normal stress coefficient, Ψ_1, versus shear rate. The Rouse model prediction for Ψ_1 in the linear regime still appears to be quite impressive. In contrast, the prediction of the UCM model seems to be quantitatively less satisfactory, although the order of magnitude is still reasonable. This result provides further evidence of the above-mentioned canceling effect in the prediction of the zero-shear viscosity by the UCM model.

The most difficult material function to predict is the second normal stress coefficient, Ψ_2, which is shown in Fig. 2(c). It should be noted that all the models except the Giesekus predict zero values of Ψ_2. As shown in Fig. 2(c), the Giesekus model can predict not only a nonzero value of Ψ_2, but also the overall behavior of Ψ_2 versus shear rate reasonably well. Another impressive capability of the Giesekus model is seen in Fig. 2(d), where it predicts the ratio of the two normal stress coefficients fairly well. {Note that it is generally known experimentally, for long-chain molecules, that $-\Psi_2/\Psi_1$ is between 0.1 and 0.4 [Doi and Edwards (1986)]}.

Overall, the best prediction of the material functions under PCF is that of the FENE-p model. However, it should be emphasized that the quantitative prediction of the linear viscoelasticity by the Rouse model is truly remarkable. Also, a reasonably good prediction by the Giesekus model for $-\Psi_2/\Psi_1$, as well as Ψ_2, seems to further support the significant role of the effect of anisotropic drag under flow.

Now let us turn to the model predictions for PEF. Figure 3 shows the results for the conformation tensor. As in the case of PCF, the Rouse model shows excellent predictions

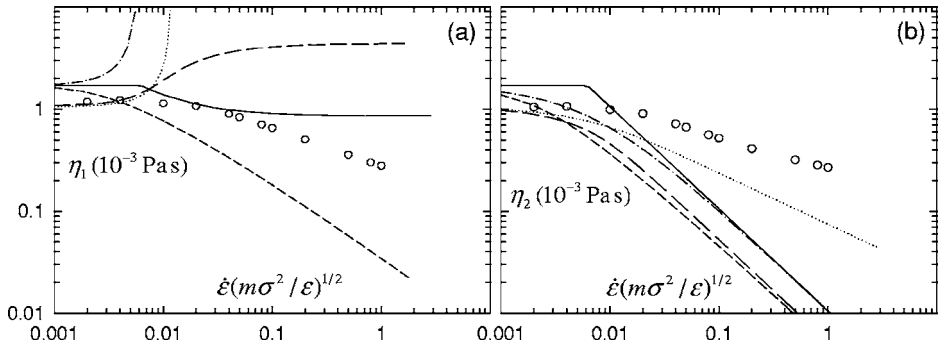

FIG. 4. Comparison between the model predictions and simulation data for the steady-state material functions for PEF: (a) first elongational viscosity and (b) second elongational viscosity. The symbols and lines represent the same quantities as in Fig. 1.

for all the components of $\tilde{\mathbf{c}}$ in the linear regime. The UCM model appears to give qualitatively, but not quantitatively, correct results for the linear data. All the nonlinear models appear to correctly predict the qualitative behaviors of $\tilde{c}_{xx}$ and $\tilde{c}_{yy}$, but the best agreement with the simulation data is observed with the FENE-p model. Notice in the figure that, as in the case of PCF, the FENE-p model predicts that all of the diagonal components go to $(b-3)/b$ in the limit of low strain rate—see Eq. (A19). An important observation is that all the models except the FENE-p predict unity for $\tilde{c}_{zz}$, as shown in Fig. 3(c). The FENE-p model appears to give fairly good predictions well up to the intermediate range of elongation rates, although the slope at the highest elongation rates appears rather steep.

In Fig. 4, the two elongational viscosities [Baig *et al.* (2005b)], η_1 and η_2, are plotted versus elongation rate. The Rouse model again very well predicts the linear viscoelastic properties, much better than the UCM model. (Both models predict tension-thickening behavior for η_1 in the nonlinear regime.) The EWM and Giesekus models capture the tension-thinning behavior of η_1 correctly, although the quantitative predictions are not very good. (Note that the Giesekus model predictions are continuous over the entire strain rate regime studied, but that the slope of the curves changes dramatically around a dimensionless strain rate of about 0.01.) On the contrary, the FENE-p model predicts a tension-thickening behavior for η_1, rather than the tension-thinning. This is considered to be a disadvantage of the FENE-p model. It is interesting to note, as shown in Fig. 4(b), that the tension-thinning behavior of η_2 is captured by all of the models, even by the linear ones. Also note that in the limit of small strain rates, the simulation data demonstrate that the zero-shear-rate viscosity [Fig. 2(a)] is equal to η_1 and η_2, in agreement with Newtonian fluid mechanics.

Overall, the predictions of nonlinear viscoelastic models for PEF do not appear to be as good as those for PCF. This is probably due to the severe stretching that occurs in elongational flow for this rather short n-alkane. Nevertheless, the Rouse model still appears to predict very well the linear viscoelasticity of PEF, as well as that of PCF.

Now let us discuss the relationship between the stress tensor, $\boldsymbol{\sigma}$, and the conformation tensor, $\tilde{\mathbf{c}}$. In the present work, all models except the FENE-p model assume a linear relationship between $\boldsymbol{\sigma}$ and $\tilde{\mathbf{c}}$. This linear relationship derived from the study of rubber elasticity assuming affine deformation of solid rubber under an external force. It has also been derived for polymer solutions or melts assuming the Gaussian chain approximation for the end-to-end vector of chains or chain segments. In Figs. 5 and 6, $\tilde{\mathbf{c}}$ is plotted versus

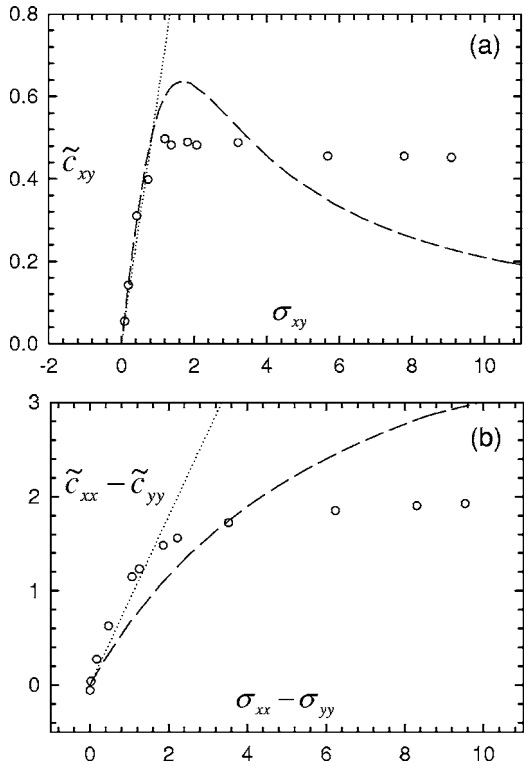

FIG. 5. The relationship between the conformation and stress tensors for PCF: (a) $\tilde{c}_{xy}$ vs σ_{xy} and (b) $\tilde{c}_{xx}-\tilde{c}_{yy}$ vs $\sigma_{xx}-\sigma_{yy}$. The circles and lines, respectively, represent the simulation data and the model predictions: the Rouse model (dotted lines) and the FENE-p model (long-dashed lines). Here, numerical values of components of the stress tensor are written in terms of the reduced units (ε/σ^3).

$\boldsymbol{\sigma}$. As shown in Fig. 5 for PCF, the linear relation appears to be valid only at small strain rates, i.e., in the linear regime. Overall, the simulation data appear to be qualitatively of the FENE-p type, Eq. (A15), rather than the straight line of Eq. (A1); i.e., the non-Gaussian effect becomes more significant with increasing shear rate. In order to better understand this behavior, the predictions from the Rouse and FENE-p model are included in the figures. The predictions of both models for the linear regime are shown to be excellent (although the prediction of the FENE-p model for $\tilde{c}_{xx}-\tilde{c}_{yy}$ seems less satisfactory than for $\tilde{c}_{xy}$). Furthermore, the FENE-p appears to perform reasonably well even for the nonlinear regime. This result seems to explain to some extent why the FENE-p model predicts PCF very well. We conjecture that this result would be valid (at least qualitatively) even for long-chain molecules as well.

The relationship between $\boldsymbol{\sigma}$ and $\tilde{\mathbf{c}}$ for PEF is shown in Fig. 6. Again, both models are observed to predict the linear data very well. Here, however, even the FENE-p-type relation between $\boldsymbol{\sigma}$ and $\tilde{\mathbf{c}}$ does not seem to be valid in this flow. This result may explain partially why the FENE-p model did not show such a good performance for PEF, as it did for PCF. Therefore, it can be concluded that a simple relationship (either linear or the FENE-p type) between $\boldsymbol{\sigma}$ and $\tilde{\mathbf{c}}$ would not be valid in general for arbitrary flows.

It is interesting to consider the simulation data for the relationship between stress and conformation, with respect to the recent work of Bach *et al.* (2003) and Luap *et al.* (2005). These groups showed that the tension-thinning regime of elongational viscosity

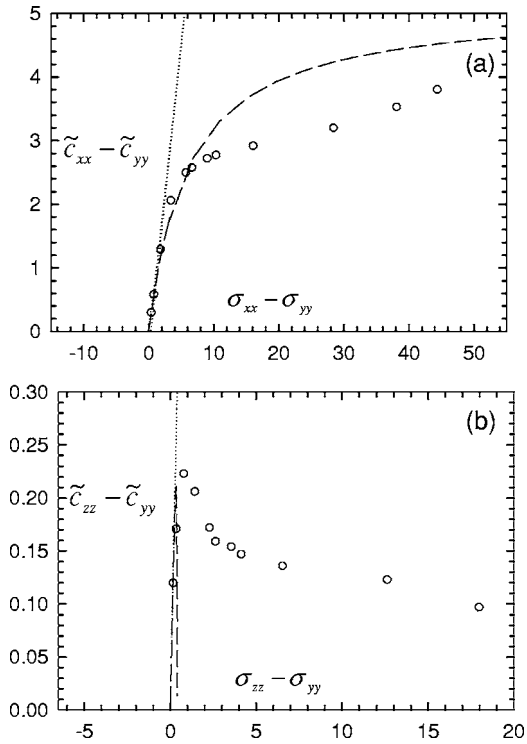

FIG. 6. The same as in Fig. 5 for PEF: (a) $\tilde{c}_{xx}-\tilde{c}_{yy}$ vs $\sigma_{xx}-\sigma_{yy}$ and (b) $\tilde{c}_{zz}-\tilde{c}_{yy}$ vs $\sigma_{zz}-\sigma_{yy}$.

extended well beyond the failure of the stress-optical relation, and so also for the onset of non-Gaussian chain stretching. Simulation data in Figs. 5 and 6 point to the same behavior, and open the possibility of examining the stress-optical relationship more thoroughly through simulations in the future.

It is also interesting to examine the above results in light of the work of Keunings (1997) concerning the Peterlin approximation of the kinetic theory FENE Model. In the FENE model, the extra stress tensor is given by the equation

$$\sigma = nK\left\langle \frac{\mathbf{RR}}{1 - R^2/R_0^2} \right\rangle. \tag{3}$$

Keunings noted that the FENE-p configurational distribution function is always Gaussian. This property is not satisfied in our simulations [Baig *et al.* (2005b)], and is a potential source of the discrepancy between the FENE-p Model and the simulation data presented above. It would be insightful to test this hypothesis by calculating the FENE stress directly from Eq. (3), without the preaveraging introduced in the FENE-p expression of Eq. (A15). Unfortunately, this calculation is too computationally intensive for us to perform reliably, since the denominator in Eq. (3) causes large fluctuations, especially as the chains extend under flow. Indeed, since we assumed that R_0^2 is based on a chain in the fully-trans conformation, it is even possible in the simulation to have a negative denominator—as the chain can acquire an extended conformation longer than R_0. Our calculations of σ using Eq. (3) appear to give more accurate descriptions of the simulation data than the FENE-p stress tensor, but we chose not to report them due to the large statistical uncertainty inherent to them. We hope to address this issue further in the future,

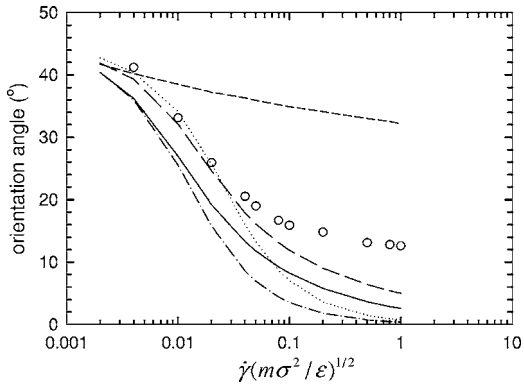

FIG. 7. Comparison between the model predictions and simulation data for the orientation angle of chains in PCF. The symbols and lines represent the same quantities as in Fig. 1.

either through much longer computations to obtain better statistics, or thorough a more thorough analysis of the non-Gaussian character of the configurational distribution function. A more meaningful value of R_0 would also help to alleviate the fluctuations in the denominator of Eq. (3).

Figure 7 depicts the comparison between the model predictions and simulation data for the orientation angle of the chains in PCF. (Note that in PEF, all model predictions and simulation data are 0° for all strain rate values.) All models except the EWM model give reasonably good predictions for this quantity. This is another sign of the inapplicability of the EWM model to short-chain molecules. The best prediction appears to be achieved by the FENE-p model.

V. SUMMARY

In view of the results presented above, the following conclusions are evident.

- Based on the results in PCF, λ(UCM) and n(UCM) are equal to approximately 0.4 $\times\lambda$(Rouse) and $2\times n$(Rouse), respectively. The excellent agreement for λ and n between simulation data and the Rouse model suggests that λ and n in this model should be considered as the true (longest) relaxation time and the "accurate" chain concentration of the system, respectively.
- The nonlinear viscoelastic models appear to perform better for PCF than PEF. The reason for this is that the degree of chain stretching and orientation is much more severe in PEF than in PCF, thus exaggerating differences between various degrees of alignment.
- The EWM model does not appear to be particularly well suited for describing the rheological and structural properties of short-chain molecular fluids. This is due to the small change in the molecular size, relative to the large change in the relaxation time induced by the model.
- Overall, the good performance of the FENE-p model for predicting nonlinear viscoelastic properties, particularly for PCF, seemed to indicate a significant role of the finite extensibility parameter, b, in short-chain dynamics. Also, the reasonable predictions of the Giesekus model—for Ψ_1, Ψ_2, and even $-\Psi_2/\Psi_1$—seem to imply the physical significance of the anisotropic drag force under flow for short-chain systems, although the extension of the chains is exaggerated.

- The well-known linear relationship between $\tilde{\mathbf{c}}$ and $\boldsymbol{\sigma}$ in polymer rheology, which only incorporates the Gaussian intramolecular entropic effect, does not seem to be valid for systems of short-chain molecules in arbitrary flows, even when the molecules are not fully stretched. For PCF, the FENE-p type equation, Eq. (A15), appears to be qualitatively valid for the relationship between $\tilde{\mathbf{c}}$ and $\boldsymbol{\sigma}$. For PEF, however, even the FENE-p type equation does not appear to be valid. In general, a more complicated relationship must apply for arbitrary flow conditions.

ACKNOWLEDGMENTS

The authors thank Dr. Vlasis Mavrantzas for his advice on, and encouragement of, this project. This research used resources of the Center for Computational Sciences at ORNL, which is supported by the Office of Science of the DOE also under Contract DE-AC05-00OR22725.

APPENDIX: PRESENTATION OF THE MODEL EQUATIONS

The UCM model contains two parameters, λ and n. The evolution equation of $\tilde{\mathbf{c}}$ and the relation between $\tilde{\mathbf{c}}$ and $\boldsymbol{\sigma}$ in the UCM model are given by [Beris and Edwards (1994)]

$$\hat{\tilde{c}}_{\alpha\beta} = -\frac{1}{\lambda}(\tilde{c}_{\alpha\beta} - \delta_{\alpha\beta}); \quad \sigma_{\alpha\beta} = nk_BT(\tilde{c}_{\alpha\beta} - \delta_{\alpha\beta}), \tag{A1}$$

where the upper-convective derivative, $\hat{\tilde{c}}_{\alpha\beta}$, is defined as

$$\hat{\tilde{c}}_{\alpha\beta} \equiv \frac{\partial \tilde{c}_{\alpha\beta}}{\partial t} + v_\gamma \nabla_\gamma \tilde{c}_{\alpha\beta} - \nabla_\gamma v_\alpha \tilde{c}_{\gamma\beta} - \tilde{c}_{\alpha\gamma} \nabla_\gamma v_\beta. \tag{A2}$$

In deriving the steady-state solutions for each model, it is useful to recognize that, in Cartesian coordinates, there are only four nonzero-independent components of $\tilde{\mathbf{c}}$ ($\tilde{c}_{xx}$, $\tilde{c}_{yy}$, $\tilde{c}_{zz}$, and $\tilde{c}_{xy}$) for PCF, and three such components ($\tilde{c}_{xx}$, $\tilde{c}_{yy}$, and $\tilde{c}_{zz}$) for PEF. By solving Eq. (A1) for PCF at steady state, the four nonzero components of $\tilde{\mathbf{c}}$ are found to be

$$\tilde{c}_{xx} = 1 + 2\lambda^2\dot{\gamma}^2; \quad \tilde{c}_{yy} = 1; \quad \tilde{c}_{zz} = 1; \quad \tilde{c}_{xy} = \lambda\dot{\gamma}. \tag{A3}$$

From Eqs. (A1) and (A3), the material functions are found to be

$$\eta_{\text{shear}}(\dot{\gamma}) = \frac{\sigma_{xy}}{\dot{\gamma}} = nk_BT\lambda; \quad \Psi_1(\dot{\gamma}) = \frac{\sigma_{xx} - \sigma_{yy}}{\dot{\gamma}^2} = 2nk_BT\lambda^2; \quad \Psi_2(\dot{\gamma}) = \frac{\sigma_{yy} - \sigma_{zz}}{\dot{\gamma}^2} = 0. \tag{A4}$$

Similarly, the three components of $\tilde{\mathbf{c}}$ and material functions for PEF are

$$\tilde{c}_{xx} = \frac{1}{1 - 2\lambda\dot{\varepsilon}}; \quad \tilde{c}_{yy} = \frac{1}{1 + 2\lambda\dot{\varepsilon}}; \quad \tilde{c}_{zz} = 1, \tag{A5}$$

$$\eta_1(\dot{\varepsilon}) = \frac{\sigma_{xx} - \sigma_{yy}}{4\dot{\varepsilon}} = \frac{nk_BT\lambda}{(1 - 2\lambda\dot{\varepsilon})(1 + 2\lambda\dot{\varepsilon})}; \quad \eta_2(\dot{\varepsilon}) = \frac{\sigma_{zz} - \sigma_{yy}}{2\dot{\varepsilon}} = \frac{nk_BT\lambda}{1 + 2\lambda\dot{\varepsilon}}. \tag{A6}$$

The Rouse model (a bead/spring chain model, where N beads are connected to each other through $N-1$ Hookean springs) also contains two independent parameters, λ and n. For $N=2$, the Rouse model reduces to the UCM model. The solutions of the conformation

tensor and material functions can be found more easily by working in terms of the normal coordinates [see Chapter 4 in Doi and Edwards (1986) for details]. The constitutive equations of $\tilde{\mathbf{c}}$ and σ are

$$\tilde{c}_{\alpha\beta} = \frac{48}{Na^2} \sum_{p:\text{odd}}^{\infty} \langle X_{p\alpha} X_{p\beta} \rangle; \quad \sigma_{\alpha\beta} = n \sum_{p=1}^{\infty} k_p \langle X_{p\alpha} X_{p\beta} \rangle - n \sum_{p=1}^{\infty} k_B T \delta_{\alpha\beta}, \tag{A7}$$

where a is the bond length between adjacent beads. The quantity $<X_{p\alpha}X_{p\beta}>$ is found by solving the evolution equation

$$\frac{\partial}{\partial t} \langle X_{p\alpha} X_{p\beta} \rangle = \frac{1}{\xi_p} (2k_B T \delta_{\alpha\beta} - 2k_p \langle X_{p\alpha} X_{p\beta} \rangle) + \nabla_\gamma v_\alpha \langle X_{p\gamma} X_{p\beta} \rangle + \nabla_\gamma v_\beta \langle X_{p\gamma} X_{p\alpha} \rangle. \tag{A8}$$

Here, X_p denotes the pth-normal mode and $\xi_p = 2N\xi$ for $p = 1, 2, 3, \ldots$, $\xi_0 = N\xi$, where ξ represents the friction constant of a bead, and p:odd represents $p = 1, 3, 5, \ldots$. The pth-mode spring constant, k_p, and relaxation time, λ_p, are defined as

$$k_p = \frac{6\pi^2 k_B T}{Na^2} p^2; \quad \lambda_p = \frac{\xi_p}{k_p} = \frac{\xi N^2 a^2}{3\pi^2 k_B T} \frac{1}{p^2} = \frac{\lambda}{p^2}, \tag{A9}$$

where λ $[\equiv \xi N^2 a^2 / (3\pi^2 k_B T)]$ represents the longest relaxation time among the modes. Solving Eq. (A8) for $<X_{p\alpha}X_{p\beta}>$ in PCF and substituting the results into Eq. (A7), the conformation tensor is found to be

$$\tilde{c}_{xx} = 1 + \frac{4}{\pi^2} \lambda^2 \dot{\gamma}^2 \sum_{p:\text{odd}} \frac{1}{p^6}; \quad \tilde{c}_{yy} = 1; \quad \tilde{c}_{zz} = 1; \quad \tilde{c}_{xy} = \frac{4}{\pi^2} \lambda \dot{\gamma} \sum_{p:\text{odd}} \frac{1}{p^4}. \tag{A10}$$

Using Eqs. (A7) and (A10), the material functions are

$$\eta_{\text{shear}}(\dot{\gamma}) = \frac{\pi^2}{12} n k_B T \lambda; \quad \Psi_1(\dot{\gamma}) = \frac{\pi^4}{180} n k_B T \lambda^2; \quad \Psi_2(\dot{\gamma}) = 0. \tag{A11}$$

Similarly, the steady-state solutions of $\tilde{\mathbf{c}}$ and material functions for PEF are

$$\tilde{c}_{xx} = \frac{8}{\pi^2} \sum_{p:\text{odd}} \frac{1}{p^2 - \lambda\dot{\varepsilon}}; \quad \tilde{c}_{yy} = \frac{8}{\pi^2} \sum_{p:\text{odd}} \frac{1}{p^2 + \lambda\dot{\varepsilon}}; \quad \tilde{c}_{zz} = 1; \tag{A12}$$

$$\eta_1(\dot{\varepsilon}) = \frac{n k_B T}{2} \lambda \sum_{p=1}^{\infty} \frac{p^2}{(p^2 - \lambda\dot{\varepsilon})(p^2 + \lambda\dot{\varepsilon})}; \quad \eta_2(\dot{\varepsilon}) = \frac{n k_B T}{2} \lambda \sum_{p=1}^{\infty} \frac{p^2}{p^2 + \lambda\dot{\varepsilon}}. \tag{A13}$$

The EWM model has the same form of the constitutive equations [Eq. (A1)] of $\tilde{\mathbf{c}}$ and $\boldsymbol{\sigma}$ as in the UCM model. However, in this model, λ is not a constant, but a function of $\tilde{\mathbf{c}}$:

$$\lambda = \lambda_0 \left(\frac{1}{3} \text{tr}\, \tilde{\mathbf{c}} \right)^k. \tag{A14}$$

The steady-state solutions of $\tilde{\mathbf{c}}$ and $\boldsymbol{\sigma}$ are easily found by replacing λ in the solutions of the UCM model with λ of Eq. (A14).

As a modified version of the UCM model, the FENE-p model contains three parameters; λ, n, and b. The constitutive equations of this model are given by

$$\hat{\tilde{c}}_{\alpha\beta} = -\frac{1}{\lambda} \left(\frac{b}{b - \text{tr}\, \tilde{\mathbf{c}}} \tilde{c}_{\alpha\beta} - \delta_{\alpha\beta} \right); \quad \sigma_{\alpha\beta} = n k_B T \left(\frac{b}{b - \text{tr}\, \tilde{\mathbf{c}}} \tilde{c}_{\alpha\beta} - \delta_{\alpha\beta} \right). \tag{A15}$$

The reduced length parameter, b, is defined as

$$b = \frac{K}{k_B T} R_0^2 = \frac{3R_0^2}{\langle R^2 \rangle_{\text{eq}}}, \tag{A16}$$

where R_0 represents the maximum allowed chain length. Taking R_0 as a fully stretched chain length with an equilibrium conformation, the calculated value of R_0 is 19.37 Å for hexadecane. $\langle R^2 \rangle_{\text{eq}}$ calculated from simulations is 219.5 Å^2. Putting these values into Eq. (A16), it is found that $b=5.13$. This value of b is used for predicting the conformation tensor and material functions for PCF and PEF. Therefore, it should be emphasized that there are no fitting parameters in this model. By solving Eq. (A15), the conformation tensor and material functions for PCF are

$$\tilde{c}_{xx} = \frac{b - \text{tr}\,\tilde{\mathbf{c}}}{b}\left[1 + 2\lambda^2\dot{\gamma}^2\left(\frac{b - \text{tr}\,\tilde{\mathbf{c}}}{b}\right)^2\right]; \quad \tilde{c}_{yy} = \tilde{c}_{zz} = \frac{b - \text{tr}\,\tilde{\mathbf{c}}}{b}; \quad \tilde{c}_{xy} = \lambda\dot{\gamma}\left(\frac{b - \text{tr}\tilde{\mathbf{c}}}{b}\right)^2, \tag{A17}$$

$$\eta(\dot{\gamma}) = nk_B T\lambda\left(\frac{b - \text{tr}\,\tilde{\mathbf{c}}}{b}\right); \quad \Psi_1(\dot{\gamma}) = 2nk_B T\lambda^2\left(\frac{b - \text{tr}\,\tilde{\mathbf{c}}}{b}\right)^2; \quad \Psi_2(\dot{\gamma}) = 0. \tag{A18}$$

Similarly, the solutions for PEF are

$$\tilde{c}_{xx} = \frac{1}{\left(\frac{b}{b - \text{tr}\,\tilde{\mathbf{c}}} - 2\lambda\dot{\varepsilon}\right)}; \quad \tilde{c}_{yy} = \frac{1}{\left(\frac{b}{b - \text{tr}\,\tilde{\mathbf{c}}} + 2\lambda\dot{\varepsilon}\right)}; \quad \tilde{c}_{zz} = \frac{b - \text{tr}\,\tilde{\mathbf{c}}}{b}, \tag{A19}$$

$$\eta_1(\dot{\varepsilon}) = \frac{nk_B T\lambda b(b - \text{tr}\tilde{\mathbf{c}})}{[b - 2\lambda\dot{\varepsilon}(b - \text{tr}\,\tilde{\mathbf{c}})][b + 2\lambda\dot{\varepsilon}(b - \text{tr}\,\tilde{\mathbf{c}})]}; \quad \eta_2(\dot{\varepsilon}) = \frac{nk_B T\lambda b(b - \text{tr}\,\tilde{\mathbf{c}})}{b + 2\lambda\dot{\varepsilon}(b - \text{tr}\,\tilde{\mathbf{c}})}. \tag{A20}$$

As the last nonlinear model in this work, the Giesekus model also contains three parameters; λ, n, and α. The parameter α, as an empirical constant, determines the strength of the anisotropic drag force in system. In order to avoid an aphysical result and not violate certain thermodynamic criteria, α should lie within the range $0 \leqslant \alpha \leqslant 1$ [Beris and Edwards (1994)]. The conformation tensor evolution equation of the Giesekus model is [Beris and Edwards (1994)]

$$\hat{c}_{\alpha\beta} = -\frac{1}{\lambda}[(1-\alpha)\delta_{\alpha\gamma} + \alpha\tilde{c}_{\alpha\gamma})](\tilde{c}_{\gamma\beta} - \delta_{\gamma\beta}); \quad \sigma_{\alpha\beta} = nk_B T(\tilde{c}_{\alpha\beta} - \delta_{\alpha\beta}). \tag{A21}$$

Notice that for $\alpha=0$, the Giesekus model reduces to the UCM model. For PCF, Eq. (A21) results in three coupled equations that must be solved simultaneously;

$$(1-2\alpha)\tilde{c}_{xx} - 2\lambda\dot{\gamma}\tilde{c}_{xy} + \alpha(\tilde{c}_{xx}^2 + \tilde{c}_{xy}^2) = 1-\alpha; \quad (1-2\alpha)\tilde{c}_{yy} + \alpha(\tilde{c}_{xy}^2 + \tilde{c}_{yy}^2) = 1-\alpha; \quad \tilde{c}_{zz} = 1;$$

$$(1-2\alpha)\tilde{c}_{xy} - \lambda\dot{\gamma}\tilde{c}_{yy} + \alpha(\tilde{c}_{xx}\tilde{c}_{xy} + \tilde{c}_{xy}\tilde{c}_{yy}) = 0. \tag{A22}$$

Thus, the material functions also need to be solved numerically. For PEF, Eq. (A21) gives rise to two uncoupled equations;

$$(1-2\alpha-2\lambda\dot{\varepsilon})\tilde{c}_{xx} + \alpha\tilde{c}_{xx}^2 = 1-\alpha; \quad (1-2\alpha+2\lambda\dot{\varepsilon})\tilde{c}_{yy} + \alpha\tilde{c}_{yy}^2 = 1-\alpha; \quad \tilde{c}_{zz} = 1, \tag{A23}$$

from which the material functions are obtained.

References

Bach, A., K. Almdal, H. K. Rasmussen, and O. Hassager, "Elongational viscosity of narrow molar mass distribution polystyrene," Macromolecules **36**, 5174–5179 (2003).

Baig, C., "Studies in rheology: Molecular simulation and theory," Ph.D. dissertation, University of Tennessee, 2005.

Baig, C., B. J. Edwards, D. J. Keffer, and H. D. Cochran, "A proper approach for nonequilibrium molecular dynamics simulations of planar elongational flow," J. Chem. Phys. **122**, 114103 (2005a).

Baig, C., B. J. Edwards, D. J. Keffer, and H. D. Cochran, "Rheological and structural studies of liquid decane, hexadecane, and tetracosane under planar elongational flow using nonequilibrium molecular dynamics simulations," J. Chem. Phys. **122**, 184906 (2005b).

Beris, A. N., and B. J. Edwards, *Thermodynamics of Flowing Systems* (Oxford University Press, New York, 1994).

Bird, R. B., R. C. Armstrong, and O. Hassager, *Dynamics of Polymeric Liquids Vol. 1, Fluid Mechanics*, 2nd ed. (Wiley-Interscience, New York, 1987a).

Bird, R. B., C. F. Curtiss, R. C. Armstrong, and O. Hassager, *Dynamics of Polymeric Liquids Vol. 2, Kinetic Theory*, 2nd ed. (Wiley-Interscience, New York, 1987b).

Cui, S. T., S. A. Gupta, P. T. Cummings, and H. D. Cochran, "Molecular dynamics simulations of the rheology of normal decane, hexadecane, and tetracosane," J. Chem. Phys. **105**, 1214–1220 (1996a).

Cui, S. T., P. T. Cummings, and H. D. Cochran, "Multiple time step nonequilibrium molecular dynamics simulation of the rheological properties of liquid n-decane," J. Chem. Phys. **104**, 255–262 (1996b).

Doi, M., and S. F. Edwards, *The Theory of Polymer Dynamics* (Oxford University Press, New York, 1986).

Edwards, B. J., C. Baig, and D. J. Keffer, "An examination of the validity of nonequilibrium molecular dynamics simulation algorithms for arbitrary steady-state flows," J. Chem. Phys. **123**, 114106 (2005).

Hoover, W. G., "Canonical dynamics: Equilibrium phase-space distributions," Phys. Rev. A **31**, 1695–1697 (1985).

Ionescu, T., C. Baig, B. J. Edwards, D. J. Keffer, and A. Habenschuss, "Structure formation under steady-state isothermal planar elongational flow of n-eicosane: A comparison between simulation and experiment," Phys. Rev. Lett. **96**, 037802 (2006).

Jeffreys, H., *The Earth: Its Origin, History and Physical Constitution* (Cambridge University Press, Cambridge, UK, 1924).

Jiang, B., P. A. Kamerkar, D. J. Keffer, and B. J. Edwards, "A test case for predicting the rheological properties of polymeric liquids: The multiple coupled Maxwell modes model," J. Non-Newtonian Fluid Mech. **120**, 11–32 (2004).

Keunings, R., "On the Peterlin approximation for finitely extensible dumbbells," J. Non-Newtonian Fluid Mech. **68**, 17–42 (1997).

Kremer, K., and G. S. Grest, "Dynamics of entangled linear polymer melts: A molecular-dynamics simulation," J. Chem. Phys. **92**, 5057–5086 (1990).

Luap, C., C. Müller, T. Schweitzer, and D. C. Venerus, "Simultaneous stress and birefringence measurements during uniaxial elongation of polystyrene melts with narrow molecular weight distribution," Rheol. Acta **45**, 83–91 (2005).

Maxwell, J. C., "On the dynamical theory of gases," Philos. Trans. R. Soc. London **157**, 49–88 (1867).

Morrison, F. A., *Understanding Rheology* (Oxford University Press, New York, 2001).

Nosé, S., "A molecular dynamics method for simulations in the canonical ensemble," Mol. Phys. **52**, 255–268 (1984a).

Nosé, S., "A unified formulation of the constant temperature molecular dynamics methods," J. Chem. Phys. **81**, 511–519 (1984b).

Oldroyd, J. G., "On the formulation of rheological equations of state," Philos. Trans. R. Soc. London, Ser. A **200**, 523–541 (1950).

Press, W. H., S. A. Teukolsky, W. T. Vetterling, and B. P. Flannery, *Numerical Recipes in Fortran 77*, 2nd ed. (Cambridge University Press, Cambridge, UK, 1992).

Siepmann, J. I., S. Karaboni, and B. Smit, "Simulating the critical behaviour of complex fluids," Nature (London) **365**, 330 (1993).